

Experimental study on minimum resolvable velocity for heterodyne laser Doppler vibrometry

Jianhua Shang (尚建华)^{1,2*}, Shuguang Zhao (赵曙光)¹, Yan He (贺岩)², Weibiao Chen (陈卫标)², and Ning Jia (贾宁)³

¹School of Information Science and Technology, Donghua University, Shanghai 201620, China

²Key Laboratory Space Laser Communication and Testing Technology, Chinese Academy of Sciences, Shanghai 201800, China

³Institute of Acoustics, Chinese Academy of Sciences, Beijing 100190, China

*Corresponding author: jhshang@dhu.edu.cn

Received January 17, 2011; accepted March 18, 2011; posted online May 31, 2011

A high spatial resolution, high velocity resolution all-fiber laser Doppler vibrometry (LDV) based on heterodyne detection for vibration measurements is reported. A linewidth of 1-kHz single-mode continuous fiber laser, polarization-preserving fiber, and a telescope with 30-mm aperture are used in this LDV. With the inphase-quadrature circuit and the digital differentiating discriminator, a high velocity resolution of 96.9 nm/s and a high displacement resolution of 2.5 pm are obtained simultaneously with a glass attached to a piezoceramic transducer. These values correspond to the measurement uncertainties of vibration velocity and displacement within 4.14% and 4.6%, respectively.

OCIS codes: 120.7280, 280.3340, 040.2840.

doi: 10.3788/COL201109.081201.

The principle of laser Doppler vibrometry (LDV) depends on the non-contacting monitoring of a Doppler shift of coherent light scatter generated by a vibrating surface, from which a time-solved vibration measurement can be obtained. The advantages of high-precision and non-destructive remote measurement provided by LDV enable it to measure the velocity and displacement of the solid objects accurately^[1–3]. LDV offers an effective alternative to traditional sensing methods, such as the accelerometers^[4]. It also presents possible applications in the dynamic testing of mechanics, on-line quality analysis, vibration controls, as well as other commercial and biomedicine fields^[5,6]. Correspondingly, the features of high sensitivity, high accuracy, as well as accurate optical alignment, complexity, and dimensions are essential consideration for the LDV application. In view of the above reasons, many comprehensive studies have attempted to improve the performance of LDV. The self-mixing LDV^[7–9], chirp heterodyne LDV^[10], and the acousto-optic frequency shifter (AOFS) heterodyne LDV^[11,12] are the main probing techniques currently being utilized.

In a previous publication^[13], we have demonstrated an LDV based on the heterodyne detection scheme. In this letter, we address some optimization operations by reducing the noise floor to develop a much higher sensitivity, eye-safe 1,550-nm all polarization-preserving fiber compact LDV, which is still based on the heterodyne coherent detection. To evaluate the performance of optimization approaches taken in the LDV, it is necessary to calibrate the measurement and performance analysis of the LDV. With a glass attached to a piezoceramic transducer (PZT) and corresponding periodic voltage driving signal, the LDV performs nano-scale velocity resolution and pico-scale spatial resolution. The results show reasonable agreement with related theories.

The implementation using LDV consisted of two parts: LDV and the calibration measurement system (Fig. 1). The LDV used to derive the velocity was separated into

the transceiver unit and the signal processing unit. The laser was centered on a 1,550-nm communication band, eye-safe, single-frequency fiber laser with the power of 30 mW and the linewidth of 1 kHz. It was divided into two paths by a beam splitter; one part acted as the transmitted laser, and the other part acted as the local oscillator (LO). In order to discriminate the direction of motion, an AOFS was equipped on the LO beam. Afterwards, the LO was frequency-shifted up by 55 MHz using the AOFS, whose driving signal served as the local oscillator signal input to the succeeding inphase-quadrature (I/Q) circuit. Through one circulator and one telescope consisting of an aspherical lens with an aperture of 30 mm, the laser incident was transmitted vertically on the glass in a calibration measurement system. The distance between the telescope and the glass was 1.5 m. The returned signal was collected by the same telescope and mixed with the LO in the beam coupler. Subsequently, the interferometric signal was detected by a balanced photodetector in order to suppress the common-mode noise during the photoelectric conversion.

During the signal process, the photodetector output

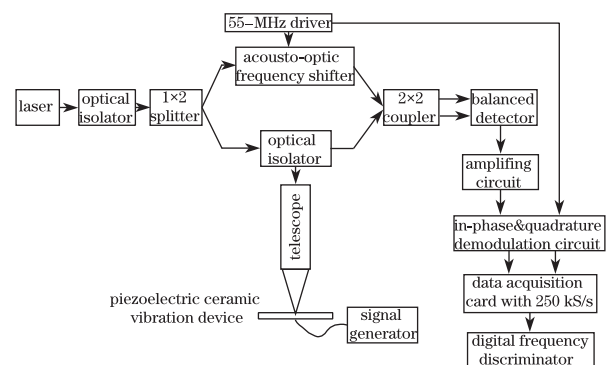


Fig. 1. Arrangement of the heterodyne LDV.

was amplified in the amplifying circuit, after which it served as the signal input to the following I/Q demodulation circuit. Equation (1) states the output analogue signal of the amplifying circuit as:

$$u(t) = \cos[2\pi f_{\text{AOFs}}t + 2\pi \int_0^t f_{\text{doppler}}(t)dt] = \cos[2\pi f_{\text{AOFs}}t + 2\pi\nu_0 \int_0^t \cos(2\pi ft)dt], \quad (1)$$

where ν_0 is the vibration velocity of the glass equals to that of PZT, and f is the vibration frequency term.

The output of the photodetector is an FM signal with a center frequency f_{AOFs} of 55 MHz, and the modulation frequency is the Doppler shift introduced by the glass vibration. In order to remove the carrier frequency f_{AOFs} , the I/Q demodulation was designed, and the output signals with a phase difference of 90° were labeled as sig_I and sig_Q. These signals containing the Doppler information were sampled by a dual-channel 250-kS/s data acquisition card. Finally, the digital differentiating discriminator reconstructed the vibration waveform of the glass directly following the processing flow described in Fig. 2. This voltage signal was proportional to the velocity of the vibrating surface as

$$u(t) = 2\pi\nu_0 \cos(2\pi ft). \quad (2)$$

In addition, the vibration frequency, velocity, and displacement of the glass vibration were also achieved. For the quantitative determination of the minimum detected vibration velocity, the calibration measurement system consists of a PZT vibration mount and a signal generator. On the surface of this vibration mount, a piece of glass is attached, which then exhibits a simple harmonic vibration. This is accompanied by the PZT, whose vibration velocity and displacement depend on its response characteristic and the driving signal characteristic.

In the most common calibration, the signal generator outputs a sine function as the driving signal to PZT. The vibration velocity of the PZT and the glass is expressed as Eq. (3), and the vibration frequency is equal to that of the sine function. Correspondingly, the minimum resolvable velocity of the LDV is the amplitude of the $v(t)$ given by

$$v(t) = 2\pi fdA \cos(2\pi ft), \quad (3)$$

where A and f are the amplitude and frequency of the driving signal, respectively, and d is the PZT strain coefficient, which is 5 nm/V in this work.

When the calibration began, the glass vibrated with the PZT according to the characteristic of the driver signal, which comprised a repeated pulse-modulated

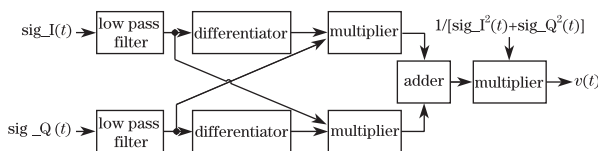


Fig. 2. Processing flow of the digital differentiating discrimination.

sine function. The amplitude and frequency of this sine function was 0.5 mV and 6 kHz, respectively, and the pulse modulation period was 1 s with a 50:50 duty cycle.

Through the time-frequency transformation of the LDV output signal related to Eq. (2), the frequency distribution of such signal was achieved (Fig. 3). Apart from the 6-kHz signal, there were 4- and 8.3-kHz signals that were distributed simultaneously. The 6-kHz signal represented the vibration frequency of the glass, with a duty ratio of 50:50 in 1 s. This is in accordance with the description of vibration shown by Eq. (2). The 4- and 8.3-kHz signals were time-continuous and stable in spectrum; they came from the performance of the processing chip in the I/Q demodulation circuit and disappeared when replaced the electronic chips. The SNR of the LDV was 16.5 dB at 6 kHz (Fig. 4). Meanwhile, below 1 kHz, the low-frequency noise occupied and agreed with the $1/f$ characteristic curve. This was demonstrated by the fact that the undesirable vibrations from the measurement environment were extremely difficult to eliminate.

The velocity resolution, which is defined as the minimum resolvable vibration velocity v_{min} of LDV, is directly proportional to the minimum detectable Doppler frequency and is calculated using Eq. (4). In this calibration measurement, a selected smaller time-domain waveform segment of the signal (Fig. 3) was obtained, whose longitudinal coordinate denotes the f_{doppler} (Fig. 4). Consequently, the minimum detected Doppler frequency increased by up to 0.125 Hz, with v_{min} of 96.9 nm/s and the corresponding minimum resolvable displacement of 2.5 pm. Comparatively, according to Eq. (3), the theoretical velocity of LDV should be 94.2 nm/s. Thus, the actual result v_{min} differed from the theoretical value by approximately +2.87% in this case.

$$v_{\text{min}} = \frac{\lambda}{2} f_{\text{doppler}_{\text{min}}}(t). \quad (4)$$

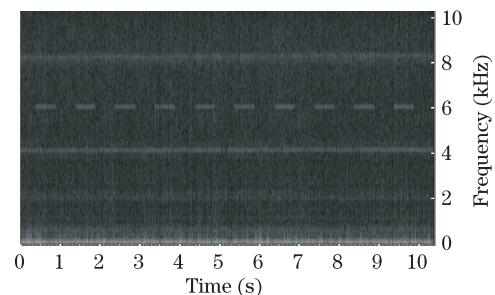


Fig. 3. Time-frequency analysis of LDV output analogue signal with PZT vibration.

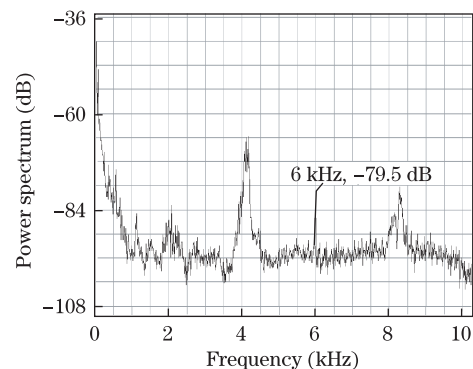


Fig. 4. Signal spectrum of LDV output with PZT vibration.

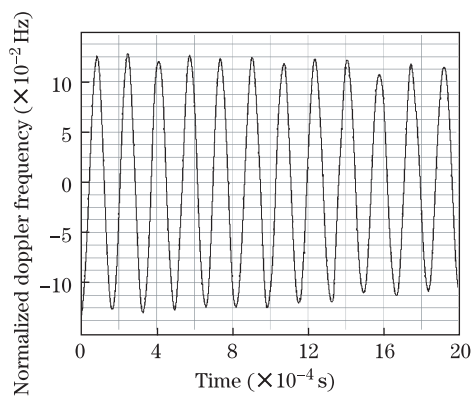


Fig. 5. LDV output signal time-domain waveform of PZT vibration.

Table 1. LDV Measuring Data and Theoretical PZT Data

Driving Voltage (mV)		Displacement (pm)	Velocity ($\mu\text{m/s}$)	Displacement Measuring Uncertainty	Velocity Measuring Uncertainty
100	LDV	494	18.60	-1.2%	-1.27%
	PZT	500	18.84		
55	LDV	278	10.46	+1.09%	+0.97%
	PZT	275	10.36		
25	LDV	123	4.65	-1.6%	-1.27%
	PZT	125	4.71		
5	LDV	24.7	0.93	-1.2%	-1.06%
	PZT	25	0.94		
2	LDV	10.3	0.39	+3%	+2.63%
	PZT	10	0.38		
0.5	LDV	2.57	96.9×10^{-3}	+2.8%	+2.87%
	PZT	2.50	94.2×10^{-3}		

The LDV detected and measured uncertainties between the detected values and theoretical values, including the vibration velocity uncertainty and the vibration displacement uncertainty under six different calibration conditions, where driving signals to PZT are varied (Table 1). The calibration results were consistent with the theoretical values, and the measuring uncertainties of vibration velocity and displacement were within 4.14% and 4.6%, respectively. According to the time-frequency analysis described in Fig. 3, the 4- and 8-kHz signals occurred simultaneously with the 6-kHz signal. These multiple Doppler shifts led to the minimum detectable Doppler frequency drifting away from the standard Doppler frequency generated only by the 6-kHz driving signal. This was also the reason why the amplitude of 6 kHz was not equal between 1.4 and 2 ms in Fig. 5. Finally, the micro deviation of the minimum detectable Doppler frequency led to the measuring uncertainty of both the measured and theoretical values.

In addition, considering a 30-m detected distance, this LDV was capable of preserving the detection sensitivity, suggesting a compromise of the long-distance remote vibration acquirement. This is generally guaranteed by

maintaining the equal optical path length in terms of the overall LO beam and transmitted beam. Furthermore, LDV can be operated real-time through the hardware design of the digital differentiating discrimination.

In conclusion, an eye-safe, high-sensitivity optimized heterodyne LDV implemented with mature communication band devices, demodulation circuits, and algorithms has been demonstrated. The calibrations of LDV performance have been presented as well. The LDV minimum resolvable vibration velocity of 96.9 nm/s and SNR of 16.5 dB have been achieved with a detected calibration vibration mount distance of 1.5 m, driving signal of 0.5 mV and 6 kHz, and telescope aperture of 30 mm. These values agree well with the theoretical results. Accordingly, the velocity and displacement measuring uncertainties are no more than 4.14% and 4.6%, respectively. In addition, the correlation between the predicted and the measured results has been confirmed. This is favorable for LDV in supporting possible innovative applications based on high-sensitivity remote vibration detections. Given the performance and minimum detectable ability of LDV, noise floor remains as the critical consideration. The nature of noise floor has been investigated and corresponding results are to be reported shortly.

The work was supported in part by the Doctoral Candidate Innovation Research Support Program of the Science & Technology Review of China (No. kjdb200902-4) and the Fundamental Research Funds for the Central University of China (No. 11D10405). The authors acknowledge the researchers from the Chinese Academy of Science for the assistance they have provided for this work.

References

1. L. E. Drain (ed.), *The Laser Doppler Technique* (Wiley-Chichester, New York, 1980), P204.
2. P. Castellini, G. M. Revel, and E. P. Tomasini, *Shock Vib. Dig.* **30**, 443 (1998).
3. F. Yang, Y. He, J. Shang, and W. Chen, *Chin. Opt. Lett.* **8**, 713 (2010).
4. C. Cristalli, N. Paone, and R. Rodríguez, *Mech. Syst. Signal Pr.* **20**, 1350 (2006).
5. P. Castellini, M. Martarelli, and E. P. Tomasini, *Mech. Syst. Signal Pr.* **20**, 1265 (2006).
6. S. Zhen, R. Liu, B. Li, J. Zhang, and B. Han, *Chin. Opt. Lett.* **7**, 26 (2009).
7. M. J. Rudd, *J. Phys. E* **1**, 723 (1968).
8. L. Scalise, Y. Yu, G. Giuliani, G. Plantier, and T. Bosch, *IEEE T. Instrum. Meas.* **53**, 223 (2004).
9. N. Servagent, T. Bosch, and M. Lescure, *IEEE T. Instrum. Meas.* **46**, 847 (1997).
10. J. Czarske and H. Müller, *Opt. Commun.* **132**, 421 (1996).
11. P. R. Kaczmarek, T. Rogowski, A. J. Antonczak, and K. M. Abramski, *Opt. Appl.* **34**, 373 (2004).
12. A. G. Mychkovsky, N. A. Chang, and S. L. Ceccio, *Appl. Opt.* **48**, 3468 (2009).
13. J. Shang, Y. He, D. Liu, H. Zang, and W. Chen, *Chin. Opt. Lett.* **7**, 732 (2009).